Published in final edited form as:
J Memb Sci. 2008 July ; 319(1-2): 192–198. doi:10.1016/j.memsci.2008.03.044.

Effect of Processing Parameters on Pore Structure and Thickness of Anodic Aluminum Oxide (AAO) Tubular Membranes

A. Belwalkar[1], **E. Grasing**[1], **W. Van Geertruyden**[2], **Z. Huang**[3], and **W.Z. Misiolek**[1]

[1]Institute for Metal Forming, Lehigh University, 5 E. Packer Ave., Bethlehem, PA 18015

[2]EMV Technologies, LLC, 116 Research Dr., Bethlehem, PA 18015, P: (610) 419-4952, e-mail: william@emvtechnologies.com

[3]Widener University, Kirkbride Hall #365A, Chester, PA 19013

Abstract

Nanoporous anodic aluminum oxide (AAO) tubular membranes were fabricated from aluminum alloy tubes in sulfuric and oxalic acid electrolytes using a two-step anodization process. The membranes were investigated for characteristics such as pore size, interpore distance and thickness by varying applied voltage and electrolyte concentration. Morphology of the membranes was examined using light optical and scanning electron microscopy and characterized using ImageJ software. Results showed that membranes having narrow pore size and uniform pore distribution with parallel channel arrays were obtained. The pore sizes were ranging from 14 to 24 nm and the wall thicknesses as high as 76 μm. It was found that the pore size increased in direct proportion with the applied voltage and inversely with the electrolyte concentration while the interpore distance increased linearly with the applied voltage. It was also observed that increase in acid concentration increased tubular membrane wall thickness that improved mechanical handling. By using anodic alumina technology, robust ceramic tubes with uniformly distributed pore-structure and parallel nano-channels of lengths and sizes practical for industrial applications were reliably produced in quantity.

Keywords

Nanoporous anodic aluminum oxide; tubular membrane; thickness; interpore distance; nanohardness

Introduction

Nanoporous Anodic Aluminum Oxide (AAO) gained exposure recently for use as a membrane in applications such as gas separation, drug delivery, and bone fixation [1–4]. The nanoporous AAO sheet membrane has been investigated for a potential application in hemodialysis by measuring the hydraulic conductivity and comparing it to those of hollow fiber polymer dialysis membranes [5]. It is known that carefully controlled anodization of aluminum in an acidic electrolyte produces a thin layer of dense aluminum oxide, followed by an ordered array of smaller-sized nanopores [6]. This self-ordered pore arrangement of the nanoporous AAO

Correspondence to: W. Van Geertruyden.

membranes with high pore densities is essential to maximize permeation and molecular flux across the membrane in a fluid separation application [7]. For example, in a hemodialysis application, a pore size that is capable of clearing small (urea, creatinine) and middle (vancomycin, inulin) molecular weight solutes while maintaining large molecular weight molecules (albumin) is the most desirable. The pore characteristics in terms of pore diameter, interpore spacing and membrane thickness are controlled by the processing parameters such as formation voltage, anodization time, electrolyte concentration and temperature [8]. Unlike currently available polymer and cellulose-based dialysis membrane, the resulting AAO tubular membrane has uniform pore size, regular pore distribution, high porosity along with good chemical resistance and temperature stability.

The fabrication of AAO sheet membranes and the relationship between processing parameters and membrane morphology has been studied previously. Recently, a highly ordered honeycomb structure was obtained in oxalic acid solution at 40 V [9,10] and in sulfuric acid at voltages ranging from 20 to 27 V [11]. It was reported that pore diameter and inter-pore spacing was linearly proportional to the applied voltage [12]. It was also proposed that self-ordering requires a porosity of 10% which is independent of the specific anodization conditions and corresponds to aluminum of about 1.2 [13]. The mechanism by which pores grow is still in debate, but pore formation models have been developed [14–18]. The pore opening of the bottom layer or barrier layer removal is also considered an important step towards making a through-hole porous anodic alumina membrane. Recently, a porous anodic alumina was detached from aluminum substrate and barrier layer was completely removed by using one–step voltage pulse detachment method [19,20]. This procedure was reported to be environmentally friendly and efficient as compared to chemical or electrochemical detachment methods [21].

Highly ordered nanoporous alumina films in sulfuric acid have also been fabricated through a single step high-field anodization. The applied potential was raised to the break-down or burning potential of the porous anodic alumina films in sulfuric acid and then increased with the aging of solutions after a long period of anodization. Self–ordering regime of nanoporous AAO was found during hard anodization (HA) of aluminum sheets in oxalic acid at the applied potentials of 100–150 V, more than thrice the voltage used in conventional oxalic acid anodization (40 V). Extremely rapid and homogeneous film growth (50–70 μm h^{-1}) was observed on the aluminum sheet sample [22,23]. Lower concentrated acid hard-coating solutions give oxide coatings that are thicker, harder, less porous, less soluble, and more wear resistant compared to higher acid concentration anodizing solutions [24].

All the above discussed techniques of mild anodization and hard anodization were performed using aluminum sheets. Aluminum tubes were anodized to form a nanoporous alumina capsules with a highly uniform and large surface area, which is relatively inexpensive device for biofiltration application [4]. Recently, cylindrical and pentagonal shaped three dimensional alumina nanotemplates were fabricated by electrochemical anodization of high-purity aluminum wires or tubes [33]. In this research, aluminum tubes were anodized in 2, 3, 5, 7, 10 and 20 wt % sulfuric acid and 2.7 wt % oxalic acid at 30 and 40 V respectively. The membranes formed under these experimental conditions were analyzed by measuring their pore size and interpore distance using ImageJ software. It has been determined that the type of acid electrolyte affected the sheet membrane morphology [25–27]. Keeping the voltage, temperature and concentration constant, when oxalic acid was used as the electrolyte, the AAO membranes were found to have more uniform nanochannels, less embodied anions and better hexagonal ordering than the membranes formed in sulfuric acid. These membranes also had larger diameter nanopores than the ones produced in sulfuric acid [5]. AAO sheets produced in sulfuric acid electrolyte were also found to have lower flexibility, hardness, and abrasion resistance than oxalic acid.

A larger tube wall thickness is an advantageous characteristic for fluid separation application as it helps to maintain the mechanical integrity of the tube during processing, handling and filtration. Conversely, a smaller tube wall thickness strengthens the rate of fluid separation by lessening the resistance to waste solute transfer across the membrane. Ideally, the membrane is as thin as possible to facilitate filtration while still retaining mechanical integrity. Such AAO tubular membranes having superior mechanical strength would able to withstand high fluid pressures and would be ideal for potential use in separation applications such as hemodialysis, plasmaspheresis and cryopreservation. In this research, the mechanical strength was investigated by measuring the membrane hardness by using nanoindentation technique.

Earlier literature describes thickness as simply a function of total charge passed to the anode [13,14]. However, others have found that thickness varies with anode geometry. It was reported that greater thickness was obtained when oxidation occurred on the inside of an aluminum tube rather than the outside [25] and this fact was incorporated in the current research.

Materials and Methods

Fabrication of nanoporous AAO tubular membranes

Nanoporous alumina tubular membranes were made from alloy 3003 aluminum ($Al_{98.6}Mn_{1.2}Cu_{0.12}$) tubes using a two-step anodization method. The length, outer diameter, and thickness of the starting tubes were 3.5cm, 6.35mm and 700μm respectively. The aluminum tubes were anodized first in 2.7 wt % oxalic acid at 30 and 40 V and the smallest pore size obtained was 18.6±2.9 nm at 30 V (table 2). Since the desired pore size was smaller than the achieved ones, sulfuric acid with different concentrations was used to produce membranes with lower pore sizes [5].

Prior to anodizing, each aluminum tube was ultrasonically cleaned in acetone for 15 minutes, followed by 5 minutes of ultrasonic cleaning in deionized water. The tube was then electropolished in a solution made up of phosphoric acid, ethanol and deionized water. This method is similar to anodization except that it uses much larger current of the order of 6.5 to 7 A for approximately 35 to 45 seconds. The electropolishing was followed by another ultrasonic cleansing in acetone and deionized water. These procedures made the sample flat, smooth with a shiny surface. The sample was then mounted on the copper rod that served as the anode. A steel rod was mounted on the copper rod as cathode. A constant voltage was used throughout the anodization process. The experimental setup is shown in Figure 1.

The sample was then anodized at a constant voltage (same as anodization voltage) for about 5–6 minutes at 0°C to grow a thin barrier oxide layer of the order of few nanometers on its surface. An acrylic polymer was applied on the grown outer barrier oxide layer. This barrier oxide played a critical role in adhering the applied polymer thereby protecting the outer aluminum surface from anodizing. This way, the anodization was carried out only on the inside of the sample tube [4].

The two-step anodization method was employed to make the pore structure regular and uniform [28]. The first anodization (appropriate acid solutions and voltage are in Table 1) was performed at 0°C for approximately 1 hour. Following the anodization, the tube was etched in a mixture of 4 wt% chromic and 8 volume % phosphoric acid at 60 °C for about thirty minutes in a hot water bath to remove the porous alumina formed during the process. The resulting inner aluminum surface contained uniform concave nano-array that was crucial for achieving ordered pore-size distribution.

Second anodization was conducted using the same voltage that was used for first anodization except for longer anodization time [31]. The typical duration for second anodization ranges

from 24 to 36 hours. A data acquisition board in conjunction with the LabVIEW program monitored the current, voltage and temperature in the anodization cell. The measured current was used to calculate the charge supplied which came out to be approximately 1800 coulombs for a 10 cm sample.

The tube was filled with deionized water, and the ends were sealed with parafilm to protect the outer ends and inside of the tube from getting etched. The polymer protecting the outer surface was then removed, by acetone. The tube was then dipped in the solution made up of one part by volume of 0.1M CuCl2 solution and four parts by volume of 10 wt % HCl that removed the unprotected aluminum in the window.

The tubes were further etched in 4% wt chromic acid and 8% volume phosphoric acid mixture for approximately 10 minutes at room temperature to remove the barrier layer from the outer surface. Finally, the parafilm end-caps were removed to drain the water out and the tube was thoroughly rinsed with water to remove any acid that might have reached inner side of the tube via nanochannels.

Characterization

Scanning electron microscopy was used to evaluate the pore diameter and interpore spacing. Mounted AAO specimens were sputtered with iridium for 4–5 seconds prior to characterization. Scanning Electron Microscopy, Light optical microscopy and a digitizing pad were employed to determine the thickness of the AAO tubular membrane.

Nanoindentation was performed using an Atomic Force Microscope (Digital Instruments, Model MMAFM-02, Nanoscope III, version 4.43r8) and Triboscope transducer (Hysitron, 1D SN5-060-71) with a 150 nm Berkovich tip installed. A trapezoidal load function with a maximum load of 200 μN was entered into the Triboscope controller software (Triboscope Load Control, version 4.1.0.0) and used to make the indent on the sample. Between 2 and 5 indents were performed for each tube's inner diameter surface. Nanoindentation was performed on tubular membranes manufactured from pure aluminum tubes. These tubes had a smaller inner diameter (2.5 mm) as compared to the aluminum alloy tubes used for measurement of pore size. However, the two-step anodization method was the same as the larger diameter tubes.

The triboscope software calculated the nanohardness by fitting the power relation to the unloading curve of the force - deflection data. The nanohardness was then calculated from the load and the projected contact area. Pore size, porosity and interpore distances were measured using NIH ImageJ software. The pore density can be calculated using the pore count given by ImageJ, or by determining the pore count by using the area fraction:

$$P=\frac{A_p}{\frac{\pi}{4}D^2} \tag{1}$$

where P is the pore count, A_p is the area fraction of pores, and D is the average pore diameter. The pore density is then determined by dividing the pore count by the selected area. For example, there are 10 full pores and 4 half pores in the square of side 'a'. Therefore, the pore density is calculated to be 12 pores per a^2. In this investigation, both methods were used to calculated pore density.

Results

The final product demonstrates the transparent AAO tubular membrane as shown in Figure 3. Total length of the tubular membrane was 6 cm whereas the effective surface area for filtration

was approximately 4.5–5 cm long. The aluminum ends were not etched and left as they were before carrying out the first anodization to aid mechanical handling. The surface and cross section view of pore structure for membranes anodized in sulfuric and oxalic acid are shown in the SEM images (Figure 4). Figure 4(a) and Figure 4(b) show the surface views of the AAO tubular membranes anodized in 5 wt% sulfuric acid at 12.5 V and in 2.7 wt% oxalic acid at 40 V respectively. Both membranes demonstrate uniformity in pore size and distribution. Thickness of the AAO tubular membrane anodized in 20 wt% sulfuric acid at 12.5 V was measured to be approximately 76 μm as shown in Figure 4(c), the aspect ratio being as high as about 3800. This result demonstrated that a very high value of aspect ratio is achievable by using the procedure described in materials and methods (See table 3 for parameters used). Figure 4(d) depicts a higher magnification cross sectional view of a tubular membrane anodized in 3 wt% sulfuric acid at 12.5 V. The figure shows pores starting at one surface (inner), extending themselves parallel to each other and ending at the other surface (outer). For example, the molecules once pass into one end (inner) of the pore would only come out from the other end (outer) of the pore without diffusing out from the middle of the pore-tunnel.

The relationship of membrane thickness and hardness with the experimental parameters was proposed. It was suggested that the mechanical strength of the nanoporous AAO tubular membrane is proportional to both the measured thickness and hardness values.

Pore Size

As shown in Figure 4(a) and 4(b), the average pore size of the tubular membranes were around 19 nm and 33 nm, when anodized in 5 wt% sulfuric acid at 12.5 V and 2.7 wt% oxalic acid at 40 V respectively. Table 2 and 3 summarize the data of pore size with respect to voltage and concentration for oxalic acid and sulfuric acid respectively. As shown in Table 2, when the voltage increased from 30 V to 40 V, the pore size increased from 18.6±2.9 to 33.6±7.6 nm respectively. Similar behavior occurred when the samples were anodized sulfuric acid at different concentrations. When voltage increased from 12.5 to 20 V in the samples anodized in 3 wt% sulfuric acid, the pore size increased from 19.9±1.9 to 24±2.5 nm respectively. In case of samples anodized in 5 wt% sulfuric acid, the pore size increased from 19.1±1.9 to 21.4 ±0.8, when the voltage increased from 12.5 to 15 V. When the concentration of sulfuric acid increased from 3 wt% to 20 wt% for the samples anodized at 12.5 V, the pore size decreased from 19.9±1.9 to 13.7±7.8 nm. The pore size of the samples anodized at 15 V decreased from 21.6±1.8 in 3 wt% sulfuric acid to 21.4±0.8 nm in 5 wt% sulfuric acid.

Interpore Distance

The interpore distances of nanoporous AAO tubular membranes anodized in sulfuric and oxalic acid are tabulated in Table 4 and 5 respectively. In case of samples anodized in 3 wt% sulfuric acid, when the voltage increased from 12.5 to 20 V, the interpore distance increased from 32.7 ±2.8 to 45.4±8 nm. The interpore distance remained constant at an average value of 31.8±1.1 nm for different concentrations of sulfuric acid at 12.5 V. A similar behavior occurred with samples anodized at 15 V in 3 wt% and 5 wt% sulfuric acid where the average interpore distance was 37.6±1.7 nm. In the case of samples anodized in 2.7 wt% oxalic acid, the interpore distances were 65.1±6.5 and 80.5±3.2 nm at 30 and 40 V, respectively.

Thickness

Figure 5 shows the graph that depicts the tubular membrane wall thickness as a function of second anodization time for 2 wt%, 10 wt% and 20 wt% sulfuric acid concentration. AAO tubular membrane thickness increased with increase in anodization time. As the anodization time increased from 2 to 32 hours, the thickness of the membrane anodized in 20 wt% sulfuric acid increased from 8.6.1±8 to 76±7 μm. Similar increase in membrane thickness was observed in case of samples anodized in 10 wt% and 3 wt% sulfuric acid with respect to anodization

time, where the membrane thickness increased from 13.7± 3.7 to 47.5±2.2 μm and from 5.5 ±0.2 to 10.3±1.3 μm respectively. It was also observed that increase in concentration of sulfuric acid increased the membrane thickness.

Hardness

The average nanohardness of select AAO tubular membrane samples is shown in Figure 6 as a function of second anodization time. Samples anodized in 2 wt %, 10 wt % and 20 wt % sulfuric acid are presented. It was observed that the membrane hardness decreased as the thickness increased with respect to time.

Discussion

Pore Size

It was found that processing parameters can have a dramatic effect on pore characteristics. The results in Table 2 and 3 indicated that the pore size of nanoporous AAO tubular membranes increased with increase in applied voltage irrespective of the electrolyte used. It is suggested that the pore formation is accompanied by volume expansion during the oxide formation at the metal-oxide interface. This volume expansion is given by Pilling-Bedworth Ratio (PBR) which is expressed as

$$\mathrm{PBR}=\frac{\text{Volume Of Oxide Produced}}{\text{Volume of Metal Consumed}} \tag{2}$$

Due to volume expansion, the oxide is pushed in tangential and in upward direction moving the oxide walls upward thereby increasing the height of the pore wall. Since higher voltage is associated with higher current densities and hence higher volume expansion, more oxide is pushed in tangential and in upward direction. The pore walls are squeezed more thereby forming larger pores.

Table 2 also indicated that the pore size decreased with increase in sulfuric acid concentration at the same voltage. Oxide growth rate and its rate of dissolution partially depended upon concentration of sulfuric acid. Higher electrolyte concentration increased oxide dissolution and oxidation growth. With faster oxidation and dissolution, the pore size decreased. Thus, pores were smaller with 20% than 3% sulfuric acid.

Interpore distance

Table 4 and 5 indicated that the interpore distance increased with increase in the applied voltage. It is well known that for AAO, the interpore distance D_{int} is linearly proportional to the applied voltage V with a proportionality constant ζ, of approximately $\zeta \approx 2.5$ nm/V

$$D_{int}=\zeta V \tag{3}$$

Table 4 indicated that the average interpore distance of the sample tubes anodized in 3% sulfuric acid at 12.5, 15 and 20 V were 32.7±2.8, 36.4±1.6 and 45±4.8 nm respectively. Using expression (3), the interpore distances at voltage 12.5, 15 and 20 V are calculated to be 31.5, 37.5 and 50 nm respectively. Thus, it is observed that the interpore distances measured by conducting the experiments are in agreement with the interpore distance calculated using the proportionality constant ζ.

From Table 4, it is also observed that the average interpore distance remains constant even when there is a change in the concentration of the electrolyte, as can be seen from the interpore

distance values of the AAO membranes yielded from different concentration of sulfuric acid at 12.5 V.

Thickness

Membrane thickness greatly affects the ability of the AAO tubular membranes to be handled, as well as decreases the probability of fracture during the fabrication process. Tube wall thicknesses obtained during this investigation ranged from 5 – 76 μm. Similarly, tube thicknesses in the literature range from 35 – 200 μm [15].

It was suggested that the dissolution of AAO in electrolyte is 'field-assisted', or strongly dependent on voltage potential [14]. Figure 5 confirms the field-assisted nature of the AAO dissolution, as increasing the acid concentration does not increase aluminum oxide dissolution. In fact, the highest acid concentration exhibits the largest membrane thickness, due to its high oxide growth rate, shown in Table 6. This is most likely caused by the variation in electrolyte conductivity, as noted by the current density experiments. The increased current gives greater impetus for greater volume expansion thereby pushing more oxide up the walls resulting in thicker membranes.

Although Figure 5 shows mostly a linear relationship between anodization time and thickness, a limiting thickness is evident with prolonged second anodization, though previous literature has suggested that the membrane thickness is proportional to total current passed to the anode [15]. This suggests that the membrane thickness is dictated by dynamic equilibrium of oxidation and chemical dissolution. The dynamic equilibrium of the oxide formation (highly dependent on the acid concentration and availability of oxygen ions) and dissolution (relatively constant due to its field-assistant nature) causes a characteristic limiting thickness. Aluminum tubes anodized in 3 wt % sulfuric acid electrolyte concentrations exhibit characteristic limiting thicknesses. The limiting wall thickness in 3wt% sulfuric acid is approximately 37 μm and occurs at 24 hours. This is due to their higher oxide growth rates which require longer anodization times to attenuate [32]. It is believed that with second anodization times longer than 32 hours, tubes anodized in 10 wt % and 20wt % sulfuric acid will also exhibit characteristic limiting thicknesses.

The dissolution of the AAO limits the tubular membrane thickness and also affects the nanohardness of the tubular membrane. Figure 6 confirms the existence of pore wall softening due to exposure to the acid electrolyte, as the nanohardness is inversely proportional to second anodization time. The pore wall softening was described previously in terms of a microcrystalline model, in which the acid electrolyte attacks the anion-rich hydrous region between the fine-grained anhydrous aluminum oxide [29]. The pore wall softening causes a decrease in nanohardness. The decrease in nanohardness confirms the domination of dissolution rate as the anodization continues.

As mentioned previously, the increase in oxidation rate is believed to be caused by an increase in conductivity. The increased conductivity increases the availability of oxygen ions and thus the oxide growth rate. The experimental results for current density, as shown in Figure 7, are in good agreement with the literature [30], which illustrates a linearly proportional relationship between 0 – 30wt % sulfuric acid.. Also shown in Table 6, the highest sulfuric acid concentration, 20 wt %, had the largest oxide growth rate.

Conclusions

In this study, AAO tubular membranes were produced under various experimental conditions and the pore size, interpore distance, thickness and hardness were measured. The voltage affected the pore size: the pore size increased with increase in the applied voltage and decreased

with increase in acid concentration. Concentration of the acids also influenced the pore size in a way that higher acid concentration increased the rate of oxidation than dissolution thereby decreasing the pore size.

Interpore distance increased with respect to the applied voltage by the proportionality constant ζ, of approximately $\zeta \approx 2.5$ nm/V. While the applied voltage was kept constant, the interpore distance remained at constant value even when the concentration of sulfuric acid was changed. It was confirmed that the interpore distance was function of the applied voltage alone.

The rate of oxide growth was found to be greater in higher acid concentrations. It was proposed that this was caused by the conductivity of the acid, as higher acid concentrations resulted in larger current densities. The field-assisted nature of the AAO dissolution was confirmed.

The membrane thickness was found to be proportional to the concentration of acidic electrolyte. However, it was also observed that prolonged second anodization time eventually reduced membrane thickness. This suggests that the membrane thickness must be described by the dynamic equilibrium of the oxidation and dissolution rates. It is proposed that the attenuation of the oxidation rate and the resulting limiting thickness is due to depletion of oxygen ions in the acid electrolyte solution. As each acid concentration exhibited a different oxidation rate, it is proposed that each acid concentration also displays a characteristic limiting thickness at a specific time, determined by the equilibrium of the oxidation rate and field-assisted dissolution rate. Besides limiting the thickness, the dissolution also affects the nanohardness of AAO tubular membranes. It was observed that the nanohardness was inversely proportional to the anodization time.

Acknowledgements

Funding for this research was provided by the National Institutes of Health Grant #1 R41 DK074254-01 and the Pennsylvania Infrastructure Technology Authority Grant# 766-07. Partial support for Dr. Wojciech Z. Misiolek has been provided by the Loewy Family Foundation.

References

1. Gorokh G, Mozalev A, Solovei D, Khatko V, Llobet E, Correig X. Anodic formation of low-aspect-ratio porous alumina films for metal-oxide sensor application. Electrochimica Acta 2006;52:1771–1780.
2. Briggs E, Walpole A, Wilshaw P, Karlsson M, Palsgard E. Formation of highly adherent nano-porous alumina on Ti-based substrates: a novel bone implant coating. J Mater Sci Mater Med 2004;15:1021–1029. [PubMed: 15448410]
3. Darder PAM, Hernandez-Velez M, Manova E, Ruiz-Hitzky E. Encapsulation of enzymes in alumina membrane of controlled pore size. Thin Solid Films 2005;495:321–326.
4. Dawai G, Yadavalli V, Paulose M, Pishko M, Grimes C. Controlled Molecular Release Using Nanoporous Alumina Capsules. Therapeutic Micro and Nanotechnology, Biomedical Microdevices 2003;5:75–80.
5. Huang Z, Zhang W, Yu J, Gao D. Nanoporous Alumina Membrane for Enhancing Hemodialysis. Journal of Medical Devices 2007;Vol.1:79–83.
6. Alwitt RS, Xu J. Stresses in sulfuric acid anodized coatings on aluminum. Journal of Electrochemistry Society 1993;140:1241–1246.
7. Chen W, Yuan J, Xia X. Characterization and Manipulation of the Electroosmotic Flow in Porous Anodic Alumina Membranes. Analytical Chemistry 2005;77:8102–8108. [PubMed: 16351161]
8. Belwalkar, A. Mechanical Engineering. PA: Widener University M.S. Thesis Chester; 2006. Experimental study of nanoporous ceramic tubes for potential application in hemodialysis; p. 127
9. Masuda H, Fukuda K. Ordered Metal Nanohole Arrays Made by a Two-Step Replication of Honeycomb Structures of Anodic Alumina. Science 1995;268:1466. [PubMed: 17843666]

10. Masuda H, Satoh M. Fabrication of gold nanodot array using anodic porous alumina as an evaporation mask. Jpn. J. Appl. Phys 1996;35:L126.
11. Masuda H, Hasegwa F. Self-ordering of Cell Arrangement of Anodic Porous Alumina Formed in Sulfuric Acid Solution. Journal of Electrochemical Society 1997;Vol. 144(No 5):L127–L130.
12. O'Sullivan JP, Wood GC. The Morphology and Mechanism of Formation of Porous Anodic Films on Aluminum. Proceedings of the Royal Society of London. Series A, Mathematical and Physical Sciences 1970;317:511–543.
13. Nielsch K, Choi J, Schwirn K, Wehrspohn R, Gosele U. Self Ordering Regimes of Porous Alumina: 10% Porosity Rule. Nano Letters 2002 July;Vol. 2(No 7):677–680.
14. Diggle JW, Downie TC, Goulding CW. Processes involved in reattainment of steady-state conditions for the anodizing of aluminum following formation voltage changes. Journal of the Electrochemical Society: Electrochemical Science 1969 June;:737–740.
15. Garcia-Vergara SJ, Skeldon P, Thompson GE, Habazaki H. A flow model of porous anodic film growth aluminum. Electrochimica Acta 2006;52:681–687.
16. Itoh N, Kato K, Tsuji T, Hongo M. Preparation of tubular anodic aluminum oxide membrane. Journal of Membrane Science 1996;117:189–196.
17. Hoar TP, Mott NF. A mechanism for the formation of porous anodic oxide films on aluminium. J. Phys. Chem. Solids 1959;9:97.
18. Siejka J, Ortega C. An O-18 Study of Field-Assisted Pore Formation in Compact Anodic Oxide Films on Al. J. Electrochem. Soc 1977;124:883.
19. Yuan JH, He FY, Sun DC, Xia XH. A Simple Method for Preparation of Through-hole Porous Anodic Alumina Membrane. Chemistry of Materials 2004;16:1841–1844.
20. Yuan JH, Chen W, Hui RJ, Hu YL, Xia XH. Mechanism of One-step Voltage Pulse Detachment of Porous Anodic Alumina Membranes. Electrochimica Acta 2006;51:4589–4595.
21. Yuan JH, Chen W, Wu JS, Lin XH, Xia XH. An Environment Friendly Electrochemical Detachment Method for Porous Anodic Alumina. Journal of Electroanalytical Chemistry 2007;600:257–264.
22. Chu S, Wada K, Inoue S, Isogai M, Yasumori A. Fabrication of Ideally Ordered Nanoporous Alumina Films and Integrated Alumina Nanotubule Arrays by High-Field Anodization. Advanced Materials 2005:2115–2119.
23. Lee W, Ji R, Gosele U, Nielsch K. Fast Fabrication of Long-range Ordered Porous Alumina Membranes by Hard-Anodization. Nature Materials 2006;Vol. 5??.
24. Sopok; Samuel. Determination of Sulfuric Acid, Oxalic Acid, and Their Matrix Effects in Aluminum Anodizing Solutions by Ion Chromatography. Defense Technical Information Center; 1988. Accession Number ADA197734,
25. Itoh NNT, Tsuji T, Hongo M. Preparation of a tubular anodic aluminum oxide membrane. Journal of Membrane Science 1998;117:189–196.
26. Patermarkis G, Masavetas K. Aluminum anodising in oxalate and sulphate solutions. Comparison of chronopotentiometric and overall kinetic response of growth mechanism of porous anodic films. Journal of Electroanalytical Chemistry 2006;588:179–189.
27. Sui Y, Saniger JM. Characterization of anodic porous alumina by AFM. Materials Letters 2001;48:127–136.
28. Jessensky O, Muller F, Gosele U. Self-organized Formation of Hexagonal Pore Arrays in Anodic Alumina. Journal of Electrochemical Society 1998;Vol. 72(10):1173–1175.
29. Alvey, CE.; Brett, MA.; Wood, GC. The mechanical properties of porous anodic aluminum oxide films on aluminum; 3rd South African Corrosion Conference; Pretoria, South Africa: CSIR Conference Centre; 1980.
30. Company Literature. Sulfuric Acid Measurement. Foxboro, MA: Foxboro; 2005.
31. Kobayashi Y, Iwasaki K, Kytonai T, Tomita A. Preparation of tubular alumina membrane with uniform straight channels by anodic oxidation process. Journal of Materials Science 1996;31:6185–6187.
32. Cherki C, Siejka J. Study by Nuclear Microanalysis and O18 Tracer Techniques of the Oxygen Transport Processes and the Growth Laws for Porous Anodic Oxide Layers on Aluminum. J. Electrochem. Soc 1973;120:784.

33. Yoo BY, Hendricks RK, Ozkan M, Myung NV. Three-dimensional Alumina Nanotemplate. Electrochimica Acta 2006;51:3543–3550.

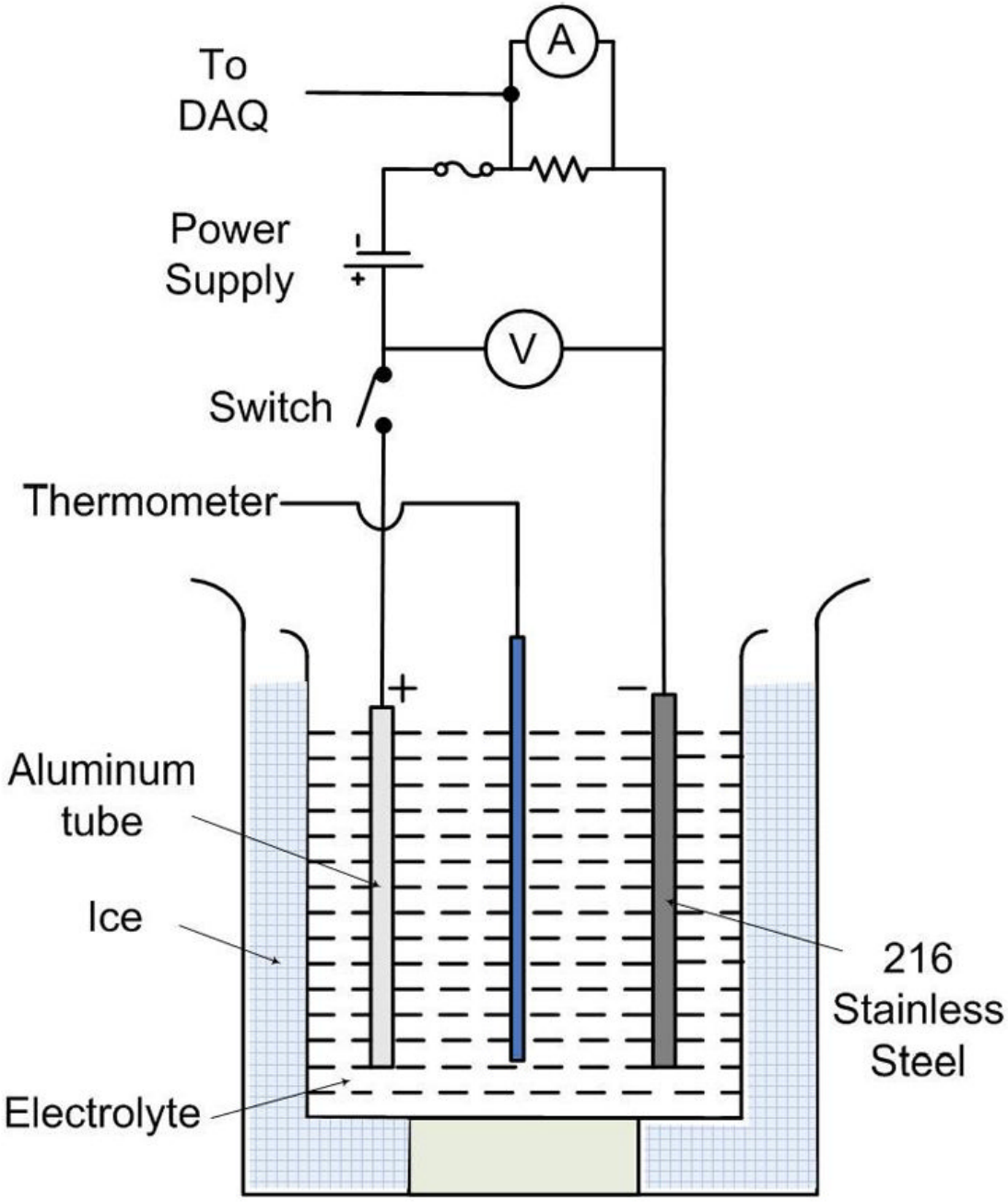

Figure 1.
Experimental setup for anodization of aluminum tubes

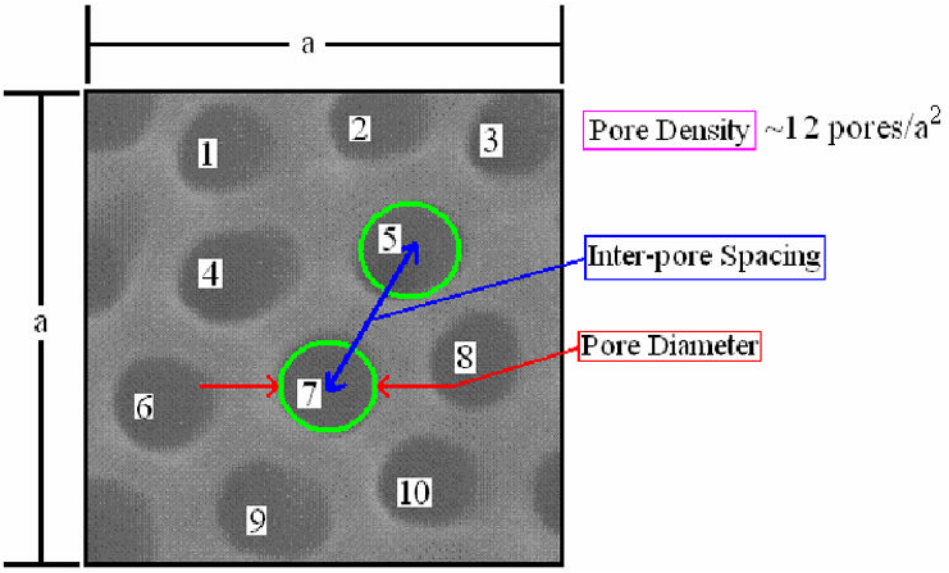

Figure 2.
Schematic illustration showing the measurement of the membrane parameters. The pore density is calculated to be 12 pores/a^2 due to the inclusion of four half pores.

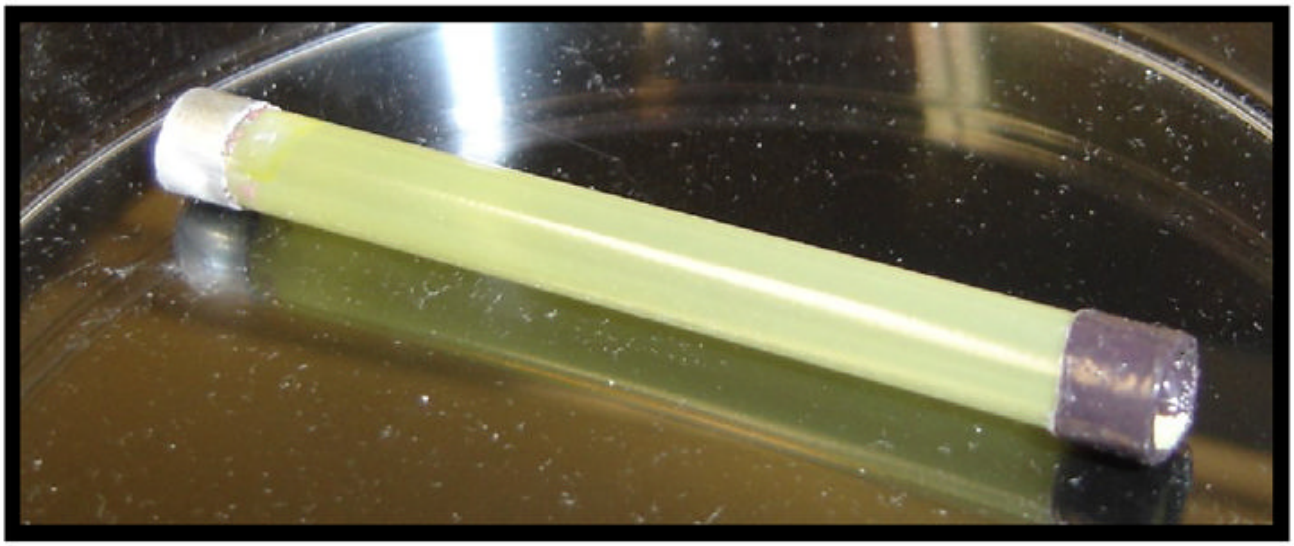

Figure 3.
Nanoporous AAO tubular membrane in its final form.

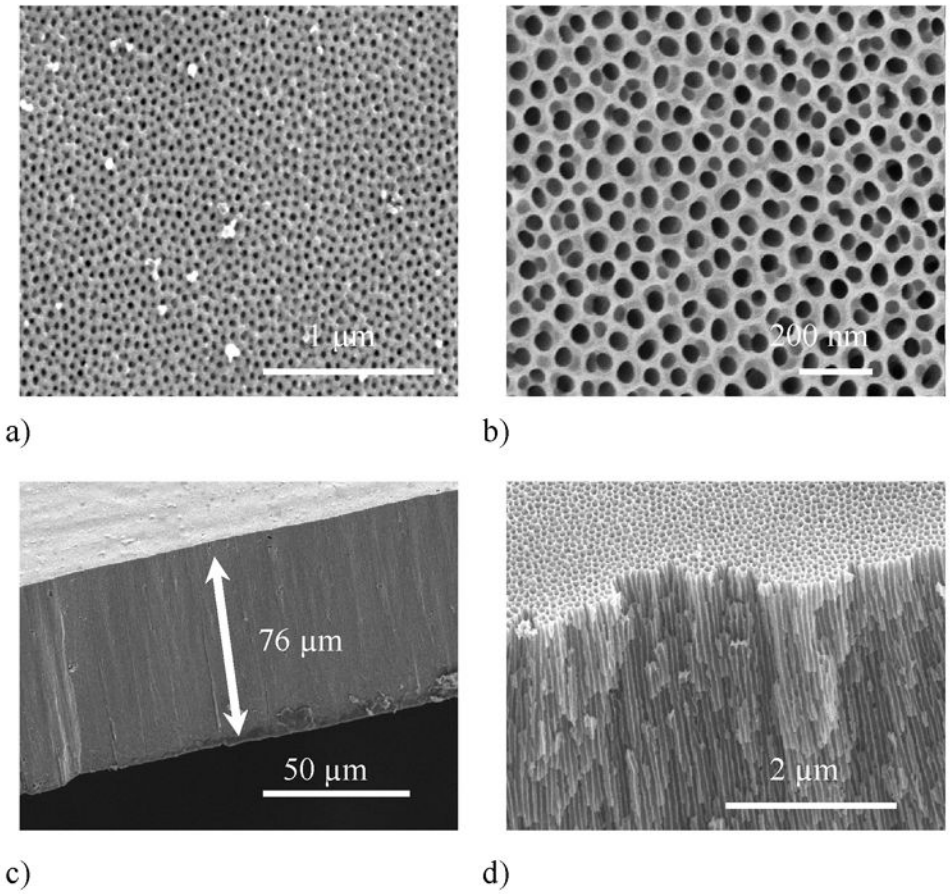

Figure 4.
SEM images of surface view of nanoporous AAO tubular membrane anodized in (a) 5 wt% sulfuric acid at 12.5 V (b) 2.7 wt% oxalic acid at 40 V. Cross section view of AAO tubular membrane anodized in (c) 20 wt% sulfuric acid at 12.5 V and (d) 3 wt% sulfuric acid at 12.5 V. Parallel nanochannels are depicted in figure 4 (d).

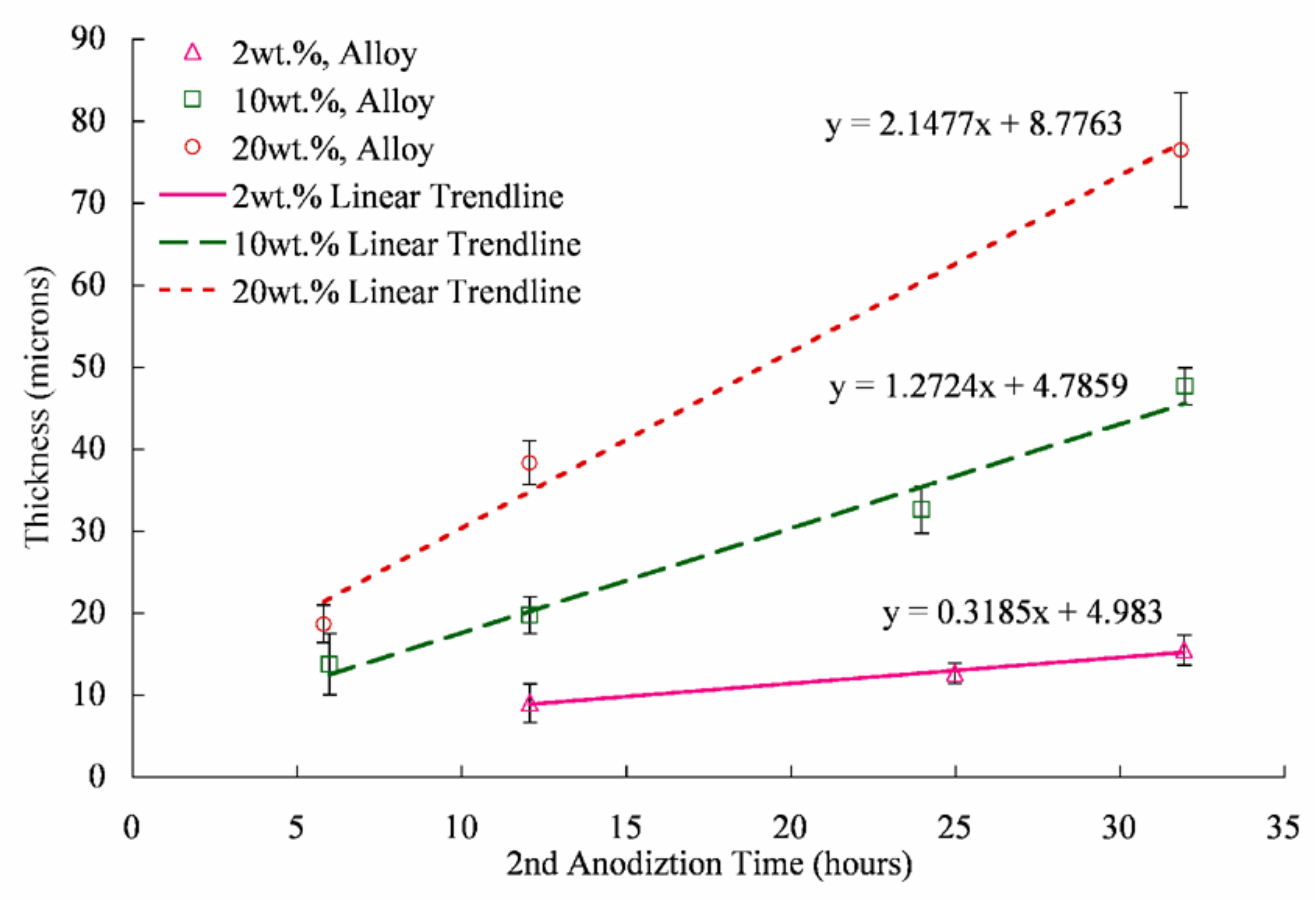

Figure 5.
Variation of AAO tubular membrane thickness with respect to anodization time.

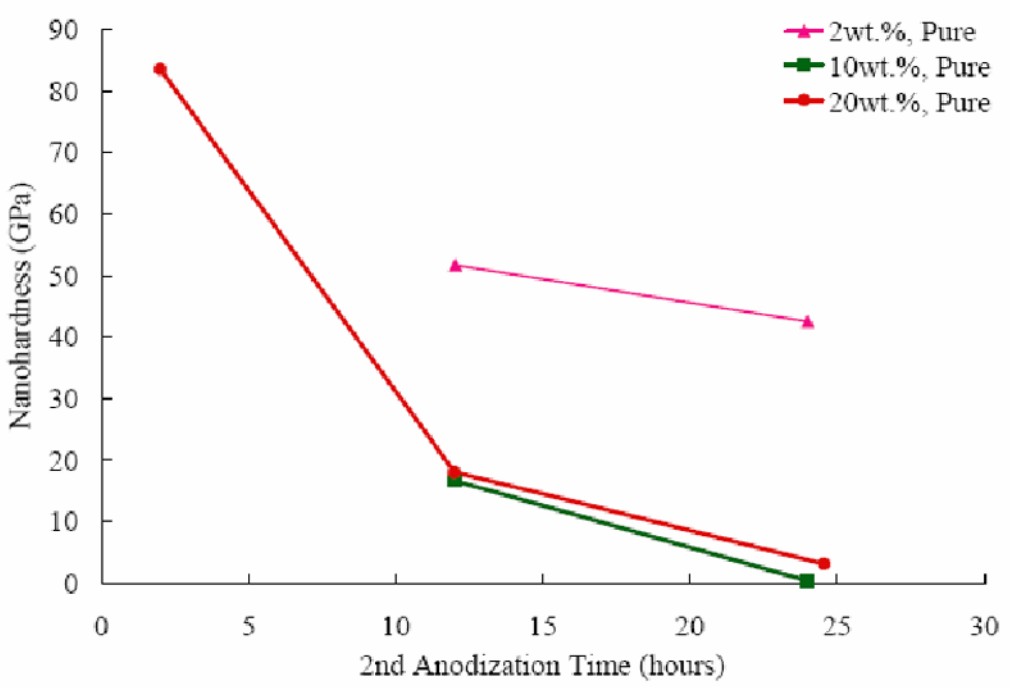

Figure 6.
The variation of nanohardness as a function of anodization time.

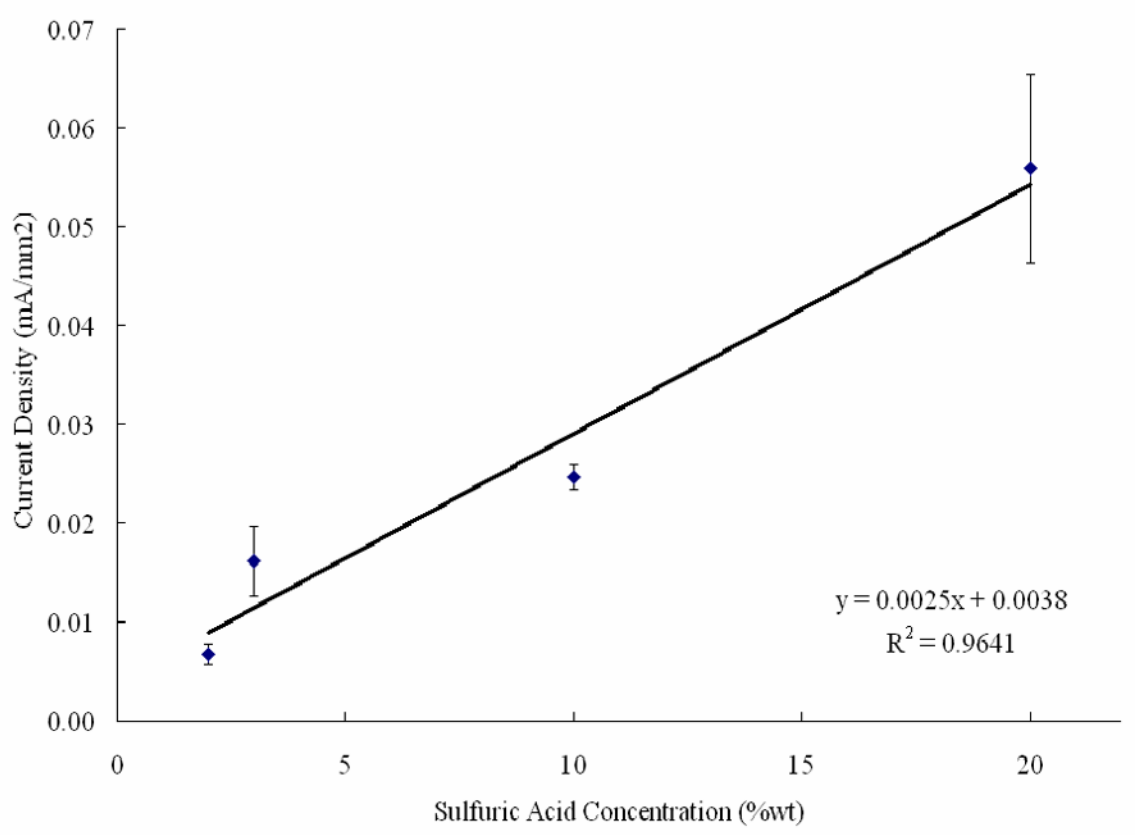

Figure 7.
Average current density during the second anodization as a function of sulfuric acid concentration.

Table 1

Experimental electrolyte solutions and applied voltages

Voltage (V)	Sulfuric Acid Concentration
12.5	2 wt%, 3 wt% , 5 wt %, 7 wt %, 10 wt %, 20 wt %
15	3 wt %, 5 wt %
20	3 wt %
Voltage (V)	Oxalic Acid Concentration
30	2.7 wt %
40	2.7 wt %

Table 2

Pore size of AAO tubular membranes produced by 2.7 wt % oxalic acid at 30 and 40 V at 0°C

Concentration of oxalic acid (wt %)	Pore Size (nm)	
	Voltage (V)	
	30	40
2.7%	18.6±2.9	33.6±7.6

Table 3

Pore size of AAO tubular membranes produced by 3 wt %, 5 wt %, 7 wt %, 10 wt % and 20 wt % sulfuric acid at 12.5, 15 and 20 V at 0°C

Concentration of sulfuric acid (wt %)	Pore Size (nm)		
	Voltage (V)		
	12.5	15	20
3	19.9±1.9	21.6±1.8	24±2.5
5	19.1±1.9	21.4±0.8	
7	19±0.5		
10	18.4±5.6		
20	13.7±7.8		

Table 4

Interpore distance of AAO tubular membranes produced by 3 wt %, 5 wt %, 7 wt %, 10 wt % and 20 wt % sulfuric acid at 12.5, 15 and 20 V at 0°C

Concentration of sulfuric acid (wt %)	Interpore Distance (nm)		
	Voltage (V)		
	12.5	15	20
3	32.7±2.8	36.4±1.6	45.4±8
5	31.9±3.2	38.8±0.4	
7	31.8±2.9		
10	32.6±4.7		
20	29.9±2.4		

Table 5

Interpore distances for AAO tubular membranes anodized by 2.7% oxalic acid at 30 and 40 V at 0°C

Concentration of oxalic acid (wt %)	Interpore Distance (nm)	
	Voltage (V)	
	30	40
2.7	65.1±6.5.	80.5±3.2

Table 6

AAO Growth rate for each sulfuric acid electrolyte concentration

Acid Concentration (wt %)	Anodic Aluminum Oxide Growth Rate (μm/hr)
2	0.318
10	1.272
20	2.148